In Situ Chemical Oxidative Graft Polymerization of Aniline from Fe_3O_4 Nanoparticles

M. Hatamzadeh[1], M. Johari-Ahar[2], M. Jaymand[2*]

1- Polymer Laboratory, Faculty of Chemistry, Payame Noor University, Tabriz, I. R. Iran
2- Research Center for Pharmaceutical Nanotechnology, Tabriz University of Medical Sciences, Tabriz, I. R. Iran

(*) Corresponding author: m_jaymand@yahoo.com

Abstract:

This study aims at exploring an effective route in the in situ graft polymerization of aniline from Fe_3O_4 nanoparticles. To this goal, Fe_3O_4 magnetic nanoparticles were prepared by coprecipitation method using ammonia solution as the precipitating agent, and were characterized by Fourier transform infrared (FT-IR) spectroscopy, X-ray diffraction (XRD) and transmission electron microscopy (TEM). Thereafter, polyaniline (PANI) grafted magnetite nanoparticles were successfully synthesized by the in situ chemical oxidative polymerization of aniline monomer by ammonium peroxodisulfate (APS) from the surfaces of the aminopropyl magnetite nanoparticles with a dispersion polymerization method. The chemical grafting of polyaniline from magnetite nanoparticles were confimed by using FT-IR, ultraviolet-visible (UV-Vis) spectroscopy and thermogravimetric analysis (TGA), and also the dispersion state of Fe_3O_4 nanoparticles in the polyaniline matrix was examined by TEM. In comparison to the pure polyaniline, the polyaniline/Fe_3O_4 nanocomposite shows to have higher decomposition temperature.

Keywords: *Magnetic nanoparticles, Surface modification, Polyaniline, In situ polymerization, Nanocomposite.*

1. INTRODUCTION

In recent years, nanoscaled magnetic particles have attracted much attention. These nanocrystallined particles with a high surface/volume ratio possess some extraordinary physical and chemical properties [1, 2]. Therefore, magnetic nanoparticles can be applied to many industrial and biological fields, such as improved MRI diagnostic contrast agents, cell separation, tumor hyperthermia, retinal detachment therapy, and magnetic field-guided carriers for localizing drugs or radioactive therapies [3-5]. A magnetic Fe_3O_4 powder, which is nontoxic and easy to be synthesized, has been intensively investigated. The preparation methods of magnetic Fe_3O_4 powders mainly include coprecipitation, microwave thermal hydrolysis, plasma thesis, laser ablation, micron-scale capsule, and glycothermal process [6,7]. However, iron black particles are naturally hydrophilic due to plentiful hydroxyls on the particle surface. Additionally, Fe_3O_4 nanoparticles, like other nanoparticles, possess high surface energy, which may result in the agglomeration of particles when Fe_3O_4 nanoparticles are dispersed in organic solvent and matrices. Therefore, the surface coating or modification of iron black particles is very important in many applications [8-10].

Composites of conducting polymers containing magnetic nanoparticles had attracted considerable attention due to their unique magnetic and electrical properties. They had many potential applications

in electrochromic device, electromagnetic interference shielding, non-linear optical systems and microwave absorbers [11-13]. Polyaniline (PANI) is a conducting polymer that shows potential for future use due to its good processibility, environmental stability, unique active conduction mechanism and reversible control of conductivity both by charge-transfer doping and protonation. Potential applications of PANI include secondary batteries, electromagnetic interference shielding, molecular sensors, nonlinear optical devices, and microelectronic devices [14-17].

Many polymerization methods have been applied to prepare magnetic polymer microspheres, such as emulsion polymerization, precipitation polymerization, and suspension polymerization. Xue *et al.* [18], obtained PANI/Fe_3O_4 nanocomposites through mechanical mixing the DBSA–PANI powder and the HCl–PANI–Fe_3O_4 powder. Wan's group [19, 20], prepared the PANI nanocomposites containing Fe_3O_4 nanoparticles by blending the PANI in N-methyl-2-pyrrolidone (NMP) with iron(II) sulfate aqueous solution, and precipitating Fe^{2+} into magnetite, and allowed the monomer to react with $FeCl_2 \cdot 4H_2O$ and $FeCl_3 \cdot 6H_2O$, following by treatment with KOH aqueous solution.

In the present work, magnetite (Fe_3O_4) nanoparticles were synthesized by chemical precipitation method. Thereafter, aniline had been in situ chemical oxidative graft from the amino groups on the surfaces of amino propyl magnetite nanoparticles directly with the facile dispersion polymerization method.

2. EXPERIMENTAL

2.1. Materials

Aniline purchased from Merck (Darmstadt, Germany), was dried with NaOH and fractionally distilled under reduced pressure from sodium or CaH_2. Ammonium peroxodissulfate (APS) from Merck was recrystallized at room temperature from EtOH/water. Analytical grade of ferric chloride hexa-hydrate ($FeCl_3 \cdot 6H_2O$), ferrous chloride tetra-hydrate ($FeCl_2 \cdot 4H_2O$), ammonium hydroxide (NH_4OH, 25% of ammonia), amino pripyl triethoxy silane (APTES), p-toluen sulphonic acid, chloform, methanol and N-methyl-2-pyrrolidone (NMP) were obtained from Merck and were used without further purification.

2.2. Synthesis of Fe_3O_4 nanoparticles

A volume of 150 mL of deionized water was placed in a round -bottomed flask; subsequently, the water was deoxygenated by bubbling N_2 gas for 30 minutes. Thereafter, 20 mL of ferrous chloride, 0.1 M, and 40 mL of ferric chloride, 0.1 M, were added. After the solution was heated to 80°C, 10 mL of NH_4OH (25% of ammonia) was rapidly added to it under vigorous stirring and immediately after, a black precipitate appeared. The resulting suspension was maintained at 80°C for 2 hours while being stirred and then cooled to room temperature. The precipitated particles are washed five times with water and methanol and dried overnight under vacuum at room temperature.

2.3. Surfaces modification of Fe_3O_4 nanoparticles by amino pripyl triethoxy silane

The introduction of -NH_2 groups onto the surface of Fe_3O_4 nanoparticles was achieved through the reaction between amino pripyl triethoxy silane (APTES) and the hydroxyl groups on the nanoparticle surface. The process started with dispersing of certain amount (1g) of Fe_3O_4 nanoparticles in the chloroform solvent (100 ml) under 20 minutes ultrasonication, into which the coupling agent APTES (1 mL) was added. The dispersed solution was then transferred to a 250 mL tree-neck round-bottom flask equipped with condenser, dropping funnel, gas inlet/outlet, and a magnetic stirrer, under bubbling N_2 gas. The solution temperature was maintained at 70°C for 12 hours under stirring and N_2 protection. The particles were recovered by centrifugation at 6000 rpm for 10 minutes. The particles were then redissolved in chloroform solvent and reprecipitated by centrifugation which was repeated until the solution was clear. The solid product was dried overnight under vacuum at room temperature.

2.4. In situ chemical oxidative polymerization of aniline from Fe_3O_4 nanoparticles

About 1 g of modified nanoparticles (Fe_3O_4-

Hatamzadeh, *et al.*

APTES) dispersed in 100 mL, p-toluen sulphonic acid (1.0 mol L^{-1}), aqueous solution of aniline (0.50 mol L^{-1}) with ultrasonic vibrations for 30 minutes. The mixture was vigorously stirred and temperature was reduced to 5°C. Thereafter, 50 mL aqueous solution of ammonium peroxodissulfate (1.10 mol L^{-1}) was drop-added into the dispersion within 30 minutes under stirring. The mixture was stirred for another 4 hours at 5°C. The product was filtered and washed with water and acetone each for three times in turn. The resulting products, polyaniline/Fe$_3$O$_4$ nanocomposite, were dried at room temperature for 48 hours under vacuum. The obtained product was extracted with N-methyl-2-pyrrolidone (NMP) in a Soxhlet apparatus for 24 hours to remove ungrafted polyaniline.

2.5. Characterization

Fourier transform infrared (FT-IR) spectra of the samples were obtained on a Shimadzu 8101M FT-IR (Shimadzu, Kyoto, Japan). The samples were prepared by grinding the dry powders with KBr and compressing the mixture to form disks. The disks were stored in a desiccator to avoid moisture absorption. The spectra were recorded at room temperature. Transmission electron microscope images (TEM) were performed on a Philips CM10-TH microscope (Phillips, Eindhoven, Netherlands) with a 100 kV accelerating voltage. The samples

used for transmission electron microscopy observations were prepared by dispersing the powders in distilled water followed by ultrasonic vibration for 15 minutes, then placing a drop of the dispersion onto a copper grid coated with a layer of amorphous carbon. X-ray diffraction (XRD) spectra was obtained with a Siemens D 5000 (Aubrey, Texas, USA), X-ray generator (CuKα radiation with λ=1.5406 Å) with a 2θ scan range of 2 to 80° at room temperature.

The thermal properties of the samples were obtained with a TGA-PL STA 1640 (Polymer Laboratories, Shropshire, UK). About 10 mg of the sample was heated between 25 and 800°C at a rate of 10°C min^{-1} under flowing nitrogen. The ultraviolet-visible (UV-Vis) spectra of the samples were measured using a Shimadzu 1601 PC, UV-Vis spectrophotometer (Shimadzu, Kyoto, Japan) in the wavelength range 300-1100 nm.

3. RESULTS AND DISCUSSION

In the present work, the magnetic nanoparticles were produced via the in situ synthesis of chemical coprecipitation technique by adding ferric (Fe^{3+}) and ferrous (Fe^{2+}) salts into the alkali solution under non oxidizing environment. This is the most common synthetic route to obtain magnetite particle compare with others, such as oxidation of Fe^{2+}, sol-
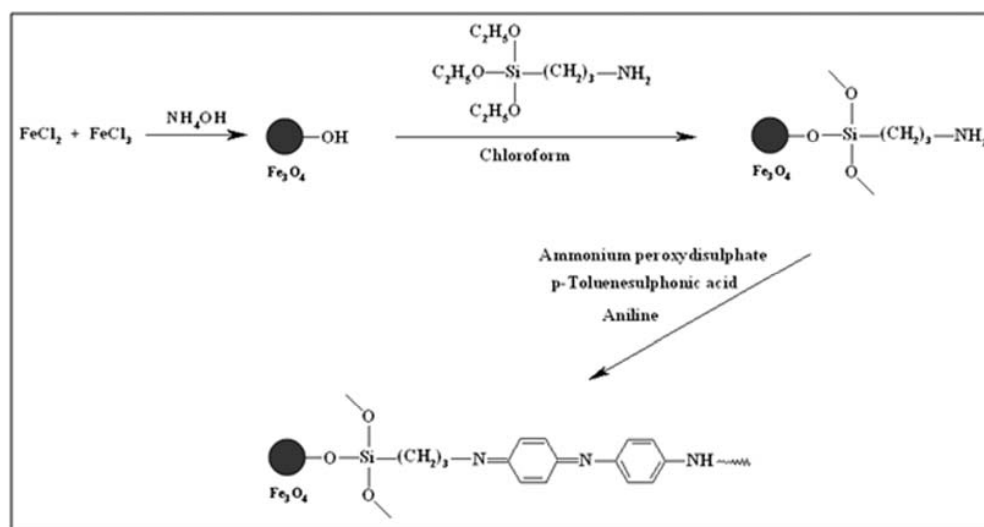
Scheme 1: *Synthetic route of the in situ chemical oxidative graft polymerization of aniline from Fe$_3$O$_4$ nanoparticles*
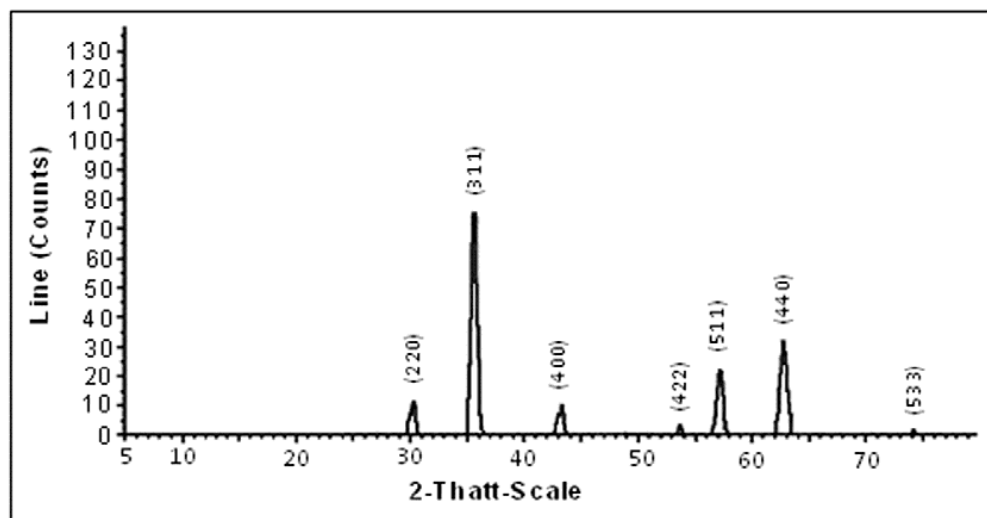
Figure 1: XRD pattern of bare Fe_3O_4 nanoparticles

gel method and water-in-oil microemulsions, in virtue of its simplicity and productivity. Thereafter, polyaniline (PANI) grafted magnetite nanoparticles were synthesized by the in situ chemical oxidative polymerization of aniline monomer with ammonium peroxodisulfate (APS) from the surfaces of the aminopropyl magnetite nanoparticles with a dispersion polymerization method. The overall methodology is summarized in Scheme 1.

3.1. Characterization of Fe_3O_4 nanoparticles

X-ray diffraction (XRD) pattern of Fe_3O_4 nanoparticles is illustrated in Figure 1. The peak intensity can be used to quantify the proportion of iron oxide forms in a mixture by comparing experimental peak and a reference peak intensity. It was found from the X-ray patterns that there were a series of characteristic peaks at 2.964 (220), 2.523 (311), 2.088 (400), 1.704 (422), 1.609 (511), 1.479 (440), and 1.276 (533).

The d values calculated from the XRD, pattern was well indexed to the inverse cubic spinel phase of Fe_3O_4. The average crystallite size D, calculated using the Debye-Scherrer formula $D=k\lambda/(\beta\cos\theta)$ was roughly about 23 nm. The equation uses the corrected reference peak width at angle θ where λ is the X-ray wavelength, β is the corrected width of the XRD peak at full width at half maximum (fwhm) and K is a shape factor which is approximated as

0.9 for magnetite.

Figure 2 shows the TEM image of the synthesized Fe_3O_4 nanoparticles. It is clear that the Fe_3O_4 nanoparticles have spherical morphology and good monodispersity. The size distribution of the Fe_3O_4 nanoparticles is narrow. However, because of the large specific surface area, high surface energy, and magnetization of Fe_3O_4 nanoparticles, some of the primary nanoparticles were aggregated into secondary particles during the process of drying.
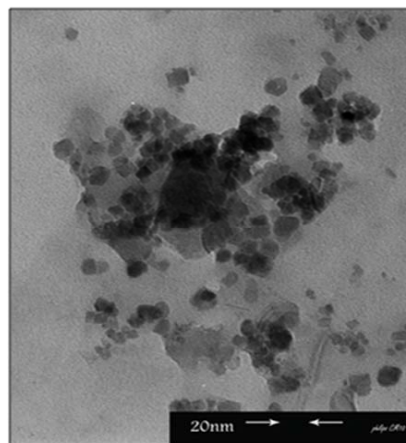
Figure 2: Transmission electron microscope image of Fe_3O_4 nanoparticles

Figure 3 shows the FT-IR spectra of unmodified (a) and modified (b) Fe_3O_4 nanoparticles. It can

Hatamzadeh, *et al.*
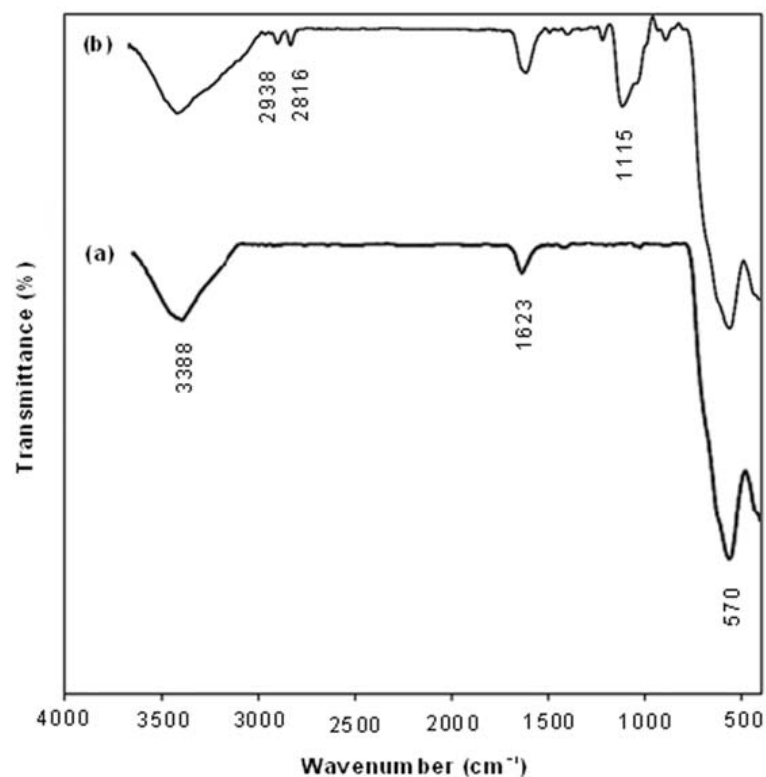
Figure 3: FT-IR spectra of unmodified Fe_3O_4 nanoparticles (a) and modified Fe_3O_4 nanoparticles by silane coupling agent (b)

be seen that the FT-IR spectrum of unmodified Fe_3O_4 nanoparticles appeared absorption bands at 570 cm^{-1} resulting from the oxygen-metal stretching vibration and the bands around 1623 and 3388 cm-1 are due to the hydroxyl groups in the Fe_3O_4 nanoparticles. FT-IR and XRD spectra confirmed that synthesis of Fe_3O_4 nanoparticles was successfully carried out.

It is well known that, in general, inorganic particles have hydroxyl groups on their surface, which can react with alkoxy silanes. Therefore, silane coupling agent is suitable for the introduction of functional groups onto the surface of inorganic particles. Figure (3-b) shows the FT-IR spectrum of modified Fe_3O_4 nanoparticles. The modification of Fe_3O_4 nanoparticles with amino pripyl triethoxy silane (APTES), confirmed by the Fe-O-Si transmittance peak at 1115 cm^{-1} and the C–H stretching vibration at 2816 and 2938 cm^{-1}.
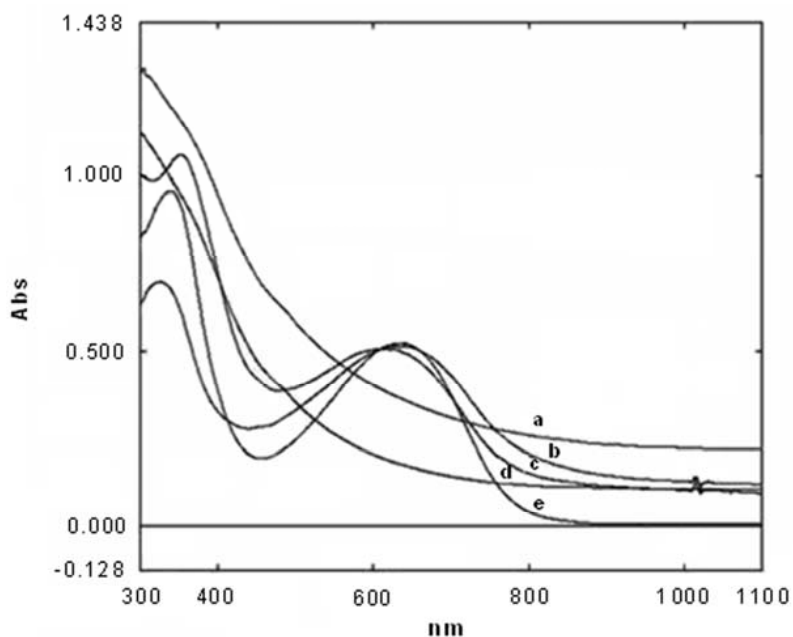
3.2. Characterization of PANI/Fe_3O_4 nano-composite

Figure 4 shows the FT-IR spectrum of PANI/ Fe_3O_4 nanocomposite. The FT-IR spectrum of nanocomposite is basically the same due to strong absorption by PANI and weak absorption of Fe_3O_4. The main characteristics peaks are assigned as follow: the band at 3472 cm^{-1} is attributable to N-H stretching mode, C=N and C=C stretching mode for the quinonoid and benzenoid units occur at 1561 and 1614 cm^{-1}. The bands around 1304 and 1218 cm^{-1} have been attributed to C-N stretching mode for benzenoid units and the band at 573 cm^{-1} is assigned to the oxygen-metal stretching vibration.

Figure 5 gives UV–Vis absorption spectra of raw Fe_3O_4 nanoparticles (d), modified nanoparticles (a), neat PANI (b), PANI/Fe_3O_4 nanocomposite before (e) and after (c) extracting with NMP solvent.
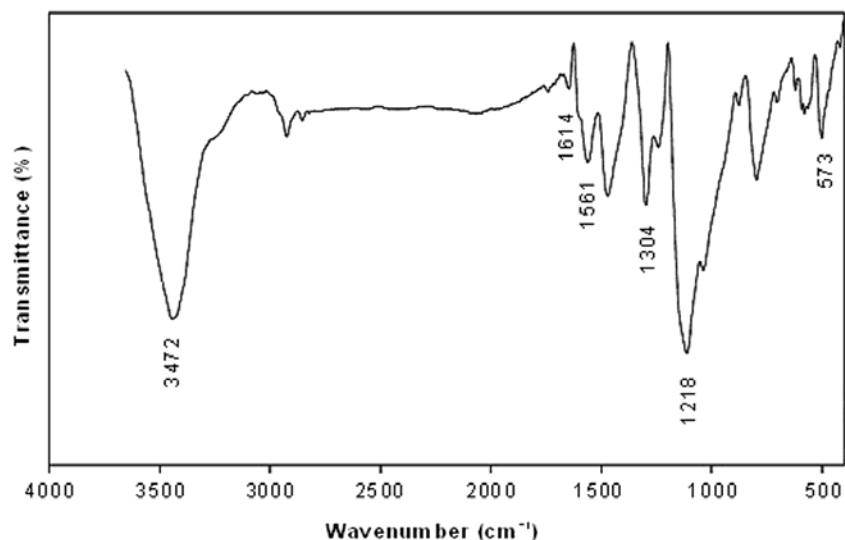
Figure 4: FT-IR spectra of PANI/Fe$_3$O$_4$ nanocomposite

Figure 5: UV-Vis spectra of modified nanoparticles (a), polyaniline (b), extracted PANI/Fe$_3$O$_4$ (c), Fe$_3$O$_4$ nanoparticles (d) and unextracted PANI/Fe$_3$O$_4$ nanocomposite (e)

Figure (6-b) shows that the PANI was characterized by two electronic transitions respectively at around 341.5 and 633.5 nm. The absorption band around 341.5 nm is attributed to π-π* transition of the benzenoid ring, while the peak around 633.5 nm corresponds to charge transfer from the benzenoid rings to the quinoid rings [14]. It is found from Figure (6-c and 6-e) that the absorption peak at 341.5 nm corresponding to PANI has a red shift in PANI/Fe$_3$O$_4$ nanocomposite, and varying degrees of red shift increase with the ferrite content the percentage of nanoparticles in nanocomposites. The percentage of nanoparticles in the PANI matrix increased with extracting of PANI/Fe$_3$O$_4$ nanocomposite with NMP solvent, because with extracting the ungrafted PANI chains removed

Hatamzadeh, *et al.*

from nanocomposite sample. These results suggest that there may be interaction between Fe_3O_4 particles and PANI chains.

3.3. Thermal stability of PANI and PANI / Fe_3O_4 nanocomposite

The characteristic thermogravimetric analysis (TGA) curves of the Fe_3O_4 nanoparticles (a), modified Fe_3O_4 nanoparticles (b), PANI/Fe_3O_4 nanocomposite (c) and pure PANI (d) are shown in Figure 6. TGA results indicate the improvement of the thermal stability for PANI/Fe_3O_4 nanocomposite compared with the neat PANI. This is different from the results of Kumar et al. [21], who found the decomposition temperature of the PANI nanocomposites with Cu_3O_4 nanoparticles was lower than that of the pure one. However, Karim et al. [22], observed that the thermal stability of PANI was relatively enhanced by forming the nanocomposites with titanium dioxide.

It seems that the influence of the inorganic nanoparticles on the thermo stability of PANI nanocomposites is very complex, its mechanism remaining to be addressed. According to the Figure (7-c), we can draw the conclusion that the weight-loss around 470-650°C in the TGA curve of PANI/Fe_3O_4 nanocomposite is a result of the decomposition of PANI covalently attached to Fe_3O_4 nanoparticles. Higher decomposition temperature of PANI/Fe_3O_4 nanocomposite (470-650°C) compared with the pure PANI (450-550°C), indicated that no polymers are noncovalently adsorbed onto the surface of Fe_3O_4 nanoparticles.

The weight loss around 200-300°C may be due to the loss of acid dopant (p-toluen sulphonic acid) bound to the polyaniline chains or the skeletal of polyaniline chains decomposed after the elimination of dopant from polymer structure. The weight percent of grafted modifier and grafted PANI are calculated from the TGA curves and summarized in Table 1.
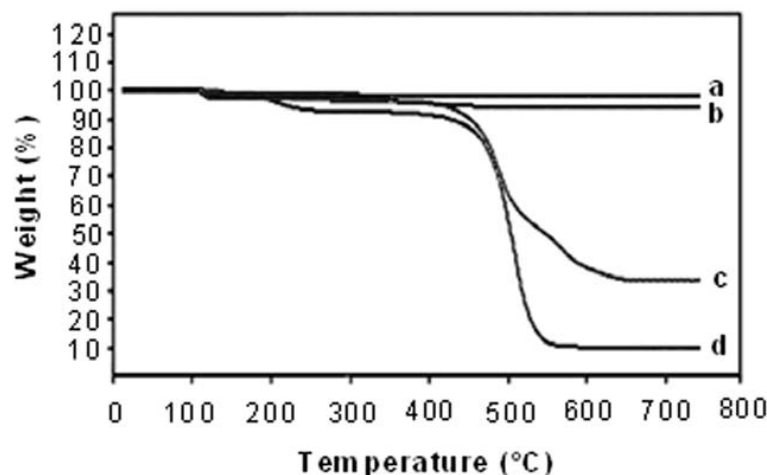

Figure 6: *TGA thermograms of bare Fe_3O_4 nanoparticles (a), modified nanoparticles (b), PANI/Fe_3O_4 nanocomposite (c) and pure PANI (d)*

Table 1: *Weight changes of the samples from TGA*

Samples	Initial wt. (%)	Residual wt. (%)	Grafted APTES (%)	Grafted PANI (%)
Fe_3O_4	100	99.14	-	-
PANI	100	9.53	-	-
Fe_3O_4-APTES	100	94.68	4.46	-
PANI/Fe_3O_4	100	33.27	4.46	61.41

3.4. Transmission electron microscopy of PANI / Fe₃O₄ nanocomposite

The obtained nanocomposite was also examined with TEM (Figure 7), which show well-dispersed Fe_3O_4 in the polyaniline matrix. Some agglomeration of Fe_3O_4 still exists, although the generally excellent separation of Fe_3O_4 particles is attributed to the growing of ''grafting from'' PANI, which separates the previously agglomerated Fe_3O_4 nanoparticles.
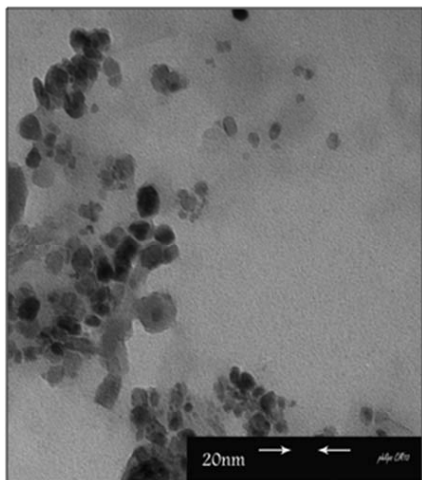
Figure 7: Transmission electron microscope image of PANI/Fe₃O₄ nanocomposite

4. CONCLUSIONS

Magnetite (Fe_3O_4) nanoparticles were synthesized by chemical precipitation. TEM image shows that the Fe_3O_4 nanoparticles have spherical morphology and good monodispersity. The PANI/Fe_3O_4 nanocomposite was synthesized by the chemical oxidative polymerization of aniline from the amino group on the surface of Fe_3O_4 nanoparticles. FT-IR, UV-Vis and TGA investigation provided direct and clear evidence for the presence of PANI shell on nano-Fe_3O_4 core particles. UV-Vis spectroscopy shows that the absorption peak at 341.5 nm corresponding to PANI has a red shift in the PANI/Fe_3O_4 nanocomposite, and varying degrees of red shift increase with the percentage of nanoparticles in nanocomposites. Thermogravimetric analysis (TGA) indicated that the resulting nanocomposite displayed higher thermal stability in comparison to the pure PANI.

ABBREVIATIONS

PANI: Polyaniline
APS: Ammonium peroxodissulfate
XRD: X-ray diffraction
TEM: Transmission electron microscopy
TGA: Thermogravimetric analysis
APTES: Amino pripyl triethoxy silane
NMP: N-methyl-2-pyrrolidone

REFERENCES

1. G. Qiu, Q. Wang, C. Wang, W. Lau, Y. Guo, Polystyrene/Fe₃O₄ magnetic emulsion and nanocomposite prepared by ultrasonically initiated miniemulsion polymerization, Ultrason. Sonochem. Vol. 14, (2007), pp. 55-61.

2. Y. Ye, Z. Pan, L. Zhang, L. He, A. Xia, H. Liang, Magnetic particle-loaded polymer brushes induced by external magnetic field: A Monte Carlo simulation, J. Polym. Sci. Part B: Polym. Phys. Vol. 48, (2010), pp. 1873-1881.

3. F. Zhang, Z. Su, F. Wen, F. Li, Synthesis and characterization of polystyrene-grafted magnetite nanoparticles, Colloid. Polym. Sci. Vol. 286, (2008), pp. 837-841.

4. R. Hao, R. Xing, Z. Xu, Y. Hou, S. Gao, S. Sun, Synthesis, Functionalization and biomedical applications of multifunctional magnetic nanoparticles, Adv. Mater. Vol. 22, (2010), pp. 2729-2742.

5. Y. Zhao, Z. Qiu, J. Huang, Preparation and analysis of Fe₃O₄ magnetic nanoparticles used as targeted drug carriers, Chin. J. Chem. Eng. Vol. 16, (2008), pp. 451-455.

6. R.Y. Hong, T. T. Pan, Y. P. Han, S. Z. Zhang, H. Z. Li, J. Ding, Graft polymerization synthesis and application of magnetic Fe_3O_4/polyacrylic acid composite nanoparticles, J. Appl. Polym. Sci. Vol. 106, (2007), pp. 1439-1447.

7. J. Sun, S. Zhou, P. Hou, Y. Yang, J. Weng, X. Li, M. Li , Synthesis and characterization of biocompatible Fe_3O_4 nanoparticles, J. Biomed. Mater. Res. Vol. 80, (2007), pp. 333-341.

8. Z. Qian, Z. Zhang, Y. Chen, A novel preparation of surface-modified paramagnetic magnetite/ polystyrene nanocomposite microspheres by radiation-induced miniemulsion polymerization, J. Colloid. Interface. Sci. Vol. 327, (2008), pp. 354-361.

9. M. Jaymand, Synthesis and characterization of well-defined poly (4-chloromethyl styrene-g-4-vinylpyridine) / TiO2 nanocomposite via ATRP technique, J. Polm. Res. Vol. 18, (2011), pp. 1617–1624.

10. D. Li, W. Y. Teoh, J. J. Gooding, C. Selomulya, R. Amal, Functionalization strategies for protease immobilization on magnetic nanoparticles, Adv. Funct. Mater. Vol. 20, (2010), pp. 1767-1777.

11. Q. Xiao, X. Tan, L. Ji, J. Xue, Preparation and characterization of polyaniline/nano-Fe_3O_4 composites via a novel Pickering emulsion route, Synth. Met. Vol. 157, (2007), pp. 784-791.

12. J. Jiang, L. Li, M. Zhu, Polyaniline/magnetic ferrite nanocomposites obtained by in situ polymerization, Reac. Funct. Polym. Vol. 68, (2008), pp. 57-62.

13. S. Wang, H. Bao, P. Yang, G. Chen, Immobilization of trypsin in polyaniline-coated nano-Fe_3O_4/carbon nanotube composite for protein digestion, Anal. Chim. Acta. Vol. 6, (2008), pp. 182-189.

14. M. Jaymand, Synthesis and characterization of conductive polyaniline-modified polymers via nitroxide mediated radical polymerization, Polymer (Korea), Vol. 34, (2010), pp. 553-559.

15. B. Massoumi, Sh. Najafian, A.A. Entezami, Investigation of conductivity and morphology of poly(diphenylamine-co-aniline) prepared via chemical and electrochemical copolymerization, Polym. Sci. Ser. B. Vol. 52, (2010), pp. 270-276.

16. S. Hanstein, A. Martinez-Bonastre, U. Nestler, P.N. Bartlett, Controlling solubility of polymeric anions in supramolecular assemblies with poly(aniline) for microsensors and actuators in human tissue, Sens. Actuators. B. Vol. 125, (2007), pp. 284-300.

17. S. H. Hosseini, Investigation of sensing effects of polystyrene-graft-polyaniline for cyanide compounds, J. Appl. Polymy. Sci. Vol. 101, (2006), pp. 3920-3926.

18. W. Xue, K. Fang, H. Qiu, J. Li, W. Mao, Electrical and magnetic properties of the Fe_3O_4-polyaniline nanocomposite pellets containing DBSA-doped polyaniline and HCl-doped polyaniline with Fe_3O_4, Synth. Met. Vol. 156, (2006), pp. 506-509.

19. M. Wan, J. Fan, Synthesis and ferromagnetic properties of composites of a water-soluble polyaniline copolymer containing iron oxide, J. Polym. Sci. Part: A. Polym. Chem. Vol. 36, (1998), pp. 2749-2755.

20. M. Wan, J. Li, Synthesis and electrical-magnetic properties of polyaniline composites, J. Polym. Sci. Part: A. Polym. Chem. Vol. 36, (1998), pp. 2799-2805.

21. V. Kumar, Y. Mastai, A. Gedanken, Sonochemical synthesis and characterization of nanocrystalline paramelaconite in polyaniline matrix, Chem. Mater. Vol. 12, (2000), pp. 3892-3895.

22. M.R. Karim, K.T. Lim, M.S. Lee, K. Kim, J. H. Yeuma, Sulfonated polyaniline-titanium dioxide nanocomposites synthesized by one-pot UV-curable polymerization method, Synth. Met. Vol. 159, (2009), pp. 209-213.

Hatamzadeh, *et al.*